V.E.2 The Effect of Airborne Contaminants on Fuel Cell Performance and Durability

Jean St-Pierre (Primary Contact), Yunfeng Zhai, Junjie Ge, Michael Angelo, Tatyana Reshetenko, Trent Molter[1], Leonard Bonville[1], Ugur Pasaogullari[1], William Collins[2], Silvia Wessel[3]

Hawaii Natural Energy Institute
1680 East-West Road
Honolulu, HI 96822
Phone: (808) 956-3909
Email: jsp7@hawaii.edu

DOE Managers

Nancy Garland
Phone: (202) 586-5673
Email: Nancy.Garland@ee.doe.gov

Reg Tyler
Phone: (720) 356-1805
Email: Reginald.Tyler@go.doe.gov

Technical Advisor

Walter Podolski
Phone: (630) 252-7558
Email: podolski@anl.gov

Contract Number: DE-EE0000467

Subcontractors:

[1] University of Connecticut, Storrs, CT
[2] UTC Power, South Windsor, CT
[3] Ballard Power Systems, Burnaby, BC, Canada

Project Start Date: April 1, 2010
Project End Date: March 31, 2014

Overall Objectives

- Identify and mitigate the adverse effects of airborne contaminants on fuel cell system performance and durability
- Provide contaminants and tolerance limits for filter specifications (preventive measure)
- Identify fuel cell stack's material, design, operation or maintenance changes to remove contaminant species and recover performance (recovery measure)

Fiscal Year (FY) 2013 Objectives

- Quantify performance loss for at least four different contaminants under various operating conditions
- Quantify spatial variability of performance loss and identify principal poisoning mechanism for at least four different contaminants

Technical Barriers

This project addresses the following technical barriers from the Fuel Cells section of the Fuel Cell Technologies Office Multi-Year Research, Development, and Demonstration Plan:

(A) Durability

(B) Cost

(C) Performance

Technical Targets

The following 2017 technical targets for automotive applications, 80-kW_e (net) integrated transportation fuel cell power systems operating on direct hydrogen, are considered:

- Durability: 5,000 hours in automotive drive cycle
- Cost: \$30 kW_e^{-1}
- Performance: 60% energy efficiency at 25% of rated power

The effects of specific airborne contaminants are studied and the resulting information will be used to impact both preventive measures and recovery procedures:

- Airborne contaminant tolerance limits to support the development of filtering system component specifications and ensure negligible fuel cell performance losses
- Fuel cell stack material, design, operation, or maintenance changes to recover performance losses derived from contamination mechanisms

FY 2013 Accomplishments

- Documented the unknown effects of seven airborne contaminants and one foreign cation on fuel cell performance and energy efficiency losses for key operating conditions (contaminant concentration, current density and temperature)
- Established tolerance limits for seven airborne contaminants and one foreign cation and 0.5, 1 and 5% performance loss levels over the target automotive fuel cell system life of 5,000 hours that offer guidance for filtering system design and cost
- Separated contaminant effects into three types of resistance losses for seven airborne species to facilitate

the selection of ex situ and in situ diagnostic techniques for mechanism determination

- Built ex situ and in situ diagnostic techniques database for seven airborne contaminants and one foreign cation to support the development of contamination mechanisms and recovery procedures that diminish the contamination impact on system durability, cost, and performance

INTRODUCTION

The composition of atmospheric air cannot be controlled and typically includes contaminants, volatile compounds, as well as ions entrained by liquid water drops in the form of rain, mist, etc., especially near marine environments. Proton exchange membrane fuel cells operated with ambient air are therefore susceptible to deleterious effects which include decreased cell performance and durability [1]. Numerous air contaminants have not yet been tested in fuel cells and consequently their effects as well as recovery methods are unknown [2]. Furthermore, prevention is difficult to achieve because tolerance limits are also missing in most cases. This increases the risk of failure for fuel cell systems and thus jeopardizes their introduction into the market.

Airborne contaminants and foreign ions have previously been selected using a cost-effective two-tiered approach combining qualitative and quantitative criteria [2]. Automotive fuel cells are used under a wide range of operating conditions resulting from changes in power demands (drive cycle). Temperature and current density impact fuel cell contamination the most [2,3]. The effect of contaminant concentration is also particularly important to assess contaminant threshold concentrations for pre-determined fuel cell performance losses and define air filtering system tolerances (prevention) [2,3]. It is likely that prevention will be insufficient to avert all contaminant effects. Therefore, recovery procedures will also be needed, and these are more easily devised by understanding the origins of the contaminant effects (mechanisms).

APPROACH

The effects of contaminants on fuel cell performance were investigated by varying operating conditions over the widest ranges possible within design specifications. Temperature was kept above 0°C, from 10 to 80°C, to avoid significant experimental complications under freezing conditions. Current density was maintained between 0.2 and 1 A cm^{-2}. The lower end of this range was sufficiently large to ensure losses are observable. Contaminant concentration was larger than the actual concentration in the atmosphere but still at trace levels to guarantee a steady state was reached relatively rapidly and a significant performance loss was perceived. The initial contaminant concentration was guessed and subsequently other contaminant concentrations were adapted based on the initial guess results. Two empirical relations were used to estimate tolerance limits from contaminant concentration dependent data and were inspired from a carbon monoxide contamination mathematical model [4].

Impedance spectroscopy was first used to classify airborne contaminant effects into different resistance losses to focus subsequent activities. As a second step, additional, more detailed information was obtained using other diagnostics methods to unravel contamination mechanisms: rotating/ring disc electrode, membrane conductivity cell, tracer method for residence time distribution measurements, segmented fuel cell for current/cell voltage distributions over the active area, and gas chromatography. Because many of these diagnostics methods are not applicable or are irrelevant to foreign ions partly due to their different state (in a liquid rather than a gaseous state) and behavior (salt precipitation within the fuel cell), other diagnostic methods were employed including photography, scanning electron microscopy and energy dispersive X-ray spectroscopy. Mathematical modeling was also exploited as experimental data obtained with many in situ diagnostic methods are subject to misinterpretations because the presence of foreign ions in the membrane and ionomer affects fuel cell resistance losses that invalidate assumptions needed to separate individual performance loss contributions [5].

RESULTS

Figure 1 summarizes the effects of temperature, current density and contaminant concentration on steady state fuel cell voltage losses for all seven airborne contaminants and one foreign cation. Cation tests were limited to 100 h for practical purposes and did not reach a steady state during this period. By contrast, airborne contaminant effects were tested for variable durations. Generally, the effect of current density was observed to be either small or more moderate than for temperature and contaminant concentration. Two outlier contaminants were noted. Bromomethane contamination was weakly affected by all operating conditions hinting at a different mechanism. The Ca^{2+} ion precipitates at a low current density of 0.2 A cm^{-2} and with operating conditions favoring cation uptake by the membrane, leading to a large performance effect.

Contaminant tolerance limits were estimated based on Figure 1c data obtained under nominal operating conditions (80°C, 1 A cm^{-2}) and using the following two empirical equations with limits of, respectively, $V_{ss,c}/V_{ss,0}$=1 and 0 for $c \rightarrow 0$ and ∞:

$$\frac{V_{ss,c}}{V_{ss,0}} = 1 - \frac{1}{1 + \frac{a}{c^b}} \quad (1)$$

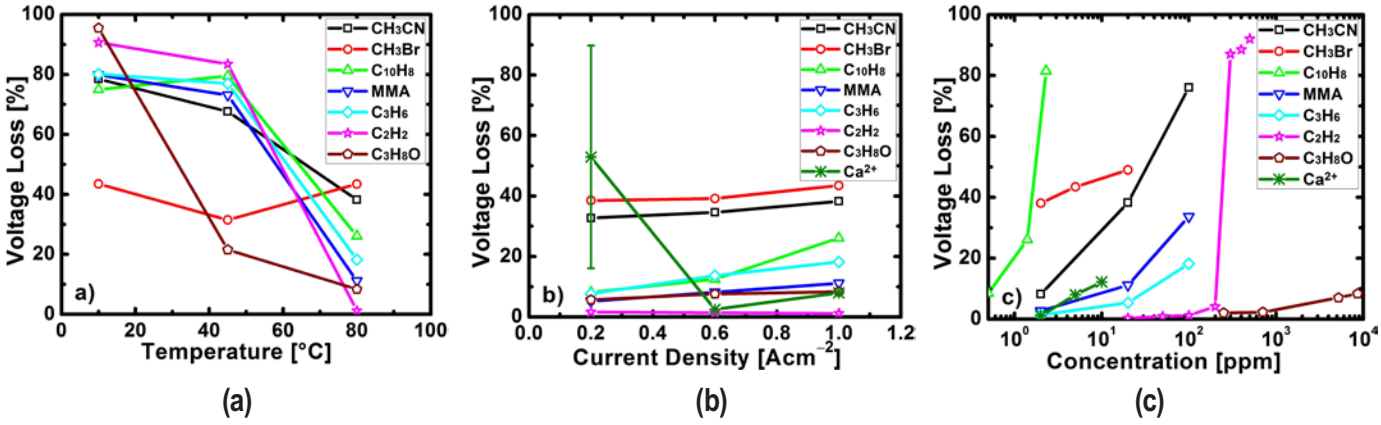

FIGURE 1. Effect of temperature (a), current density (b) and contaminant concentration (c) on fuel cell performance losses resulting from an exposure to seven airborne contaminants (at steady state) and one foreign cation (≤100 h exposure). CH_3CN: acetonitrile, CH_3Br: bromomethane, $C_{10}H_8$: naphthalene, MMA: methyl methacrylate, C_3H_6: propylene, C_2H_2: acetylene, C_3H_8O: iso-propanol.

$$\frac{V_{ss,c}}{V_{ss,0}} = 1 - \frac{1}{1 + \frac{a}{e^{bc} - 1}} \quad (2)$$

where $V_{ss,c}$ is the steady-state cell voltage during contamination (100 h value for Ca^{2+}), $V_{ss,0}$ is the steady-state cell voltage before contamination, c is the contaminant concentration and, a and b are fitted parameters. Equation 2 was used for most contaminants whereas Equation 1 was employed for bromomethane because it leads to a more gradual change with concentration. All contaminant tolerance limits and equation parameters are given in Table 1 with r^2 representing the curve fit correlation coefficient. It is implied that a steady state is reached within the 5,000 hours automotive system life. The confidence level in these contaminant tolerance limits is color coded: high in green (located within the experimental contaminant concentration range), medium in yellow (smaller than the lower end of the experimental contaminant concentration range by a factor approximately less than 10) and low in red (much smaller than the lower end of the experimental contaminant concentration range). A tolerance limit of 380 ppm has already been deduced for Ca^{2+} by a mathematical model [5], which is significantly larger than the corresponding value of 0.71 ppm based on experimental data (Table 1). The difference is expected because the model only takes into account a single mechanism for the performance loss (membrane resistance) whereas experimental data include all sources of performance loss.

A validated SO_2 contamination equivalent electrical circuit model was used [6] to extract key resistance losses from impedance spectra obtained with all seven airborne contaminants (Figure 2). Generally, changes in both kinetic (oxygen reduction reaction, R_c) and mass transfer resistances (R_d) are observed. By contrast, only acetonitrile leads to ohmic resistance R losses (membrane, ionomer). These findings indicate that multiple steps in recovery procedures may be needed as more than one type of resistance loss for

TABLE 1. Contaminant Tolerance Limits for 5, 1 and 0.5 % Fuel Cell Performance Losses

Contaminant	Predicted contaminant tolerance (ppm)			Experimental contaminant concentration range (ppm)	Empirical correlation parameters		
	$V_{ss,c}/V_{ss,0}$=0.95	$V_{ss,c}/V_{ss,0}$=0.99	$V_{ss,c}/V_{ss,0}$=0.995		*a*	*b*	r^2
Acetonitrile	1.7	0.33	0.16	2-100	9.03×10^{-5}	2.80×10^{-6}	0.995
Acetylene	210	170	158	20-500	611,000	0.0507	0.994
Bromomethane	5.7×10^{-6}	1.1×10^{-9}	3.0×10^{-11}	2-20	1.84	0.193	0.995
Iso-propanol	4,200	800	400	250-8,600	8.53×10^{-5}	1.07×10^{-9}	0.857
Methyl methacrylate	9.9	1.9	0.95	2-100	4.03×10^{-6}	2.13×10^{-8}	0.988
Naphthalene	0.63	0.21	0.12	0.5-2.4	59.2	2.26	0.987
Propene	23	4.5	2.2	2-100	6.86×10^{-6}	1.56×10^{-8}	0.978
Ca^{2+}	3.7	0.71	0.35	2-10	2.13×10^{-7}	3.05×10^{-9}	0.925

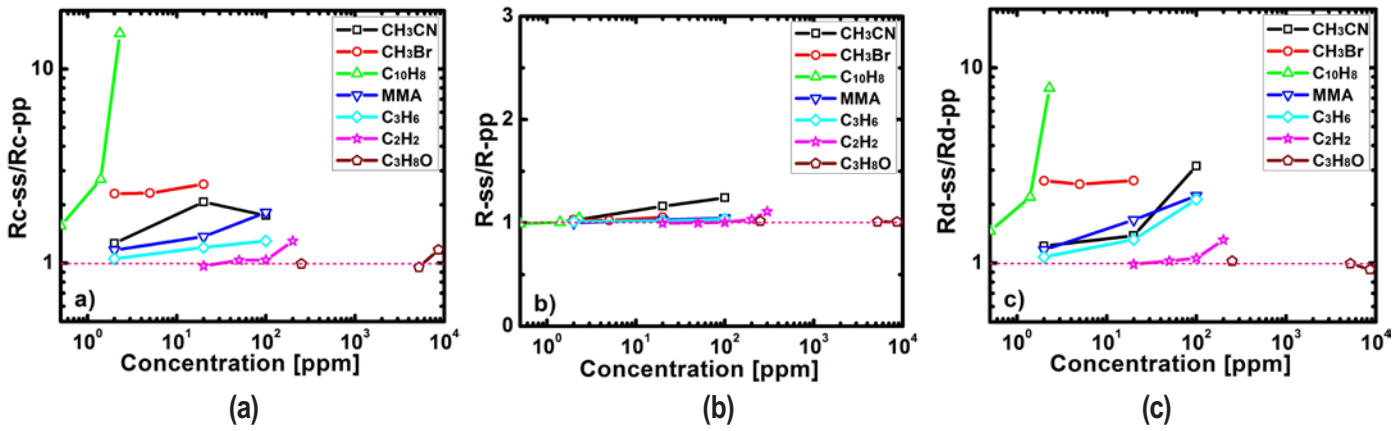

FIGURE 2. Dimensionless ratios of steady-state equivalent circuit model resistances during contamination (ss subscript) to pre-poisoning (pp subscript) values. Oxygen reduction reaction resistance R_c (a), membrane resistance R (b) and generalized finite length Warburg element resistance R_d (c). CH_3CN: acetonitrile, CH_3Br: bromomethane, $C_{10}H_8$: naphthalene, MMA: methyl methacrylate, C_3H_6: propylene, C_2H_2: acetylene, C_3H_8O: iso-propanol.

each contaminant is common. Furthermore, kinetic and mass transfer resistance changes are linked because their behaviors are quite similar as a function of contaminant concentration. It is hypothesized that contaminant adsorption on the catalyst surface decreases the active area and lengthens the oxygen mass transfer path to reach uncovered catalyst sites.

Additional data to resolve contamination mechanisms were obtained using other diagnostic methods for all seven airborne contaminants and one foreign cation. Results are summarized in Table 2. From a kinetic resistance standpoint, rotating ring/disc electrode results generally reveal that airborne contaminants decrease the catalyst active area (electrochemical catalyst area) and also modify the oxygen reduction reaction mechanism with an increase in the peroxide production side reaction (H_2O_2 current). The net effect of these changes is a poorer catalyst performance (kinetic current) and a greater risk of ionomer or membrane degradation by radical attack. The rotating ring/disc electrode is not directly applicable to the Ca^{2+} contaminant. The relatively high acid concentration needed to minimize the ohmic drop correction disturbs the Ca^{2+}/H^+ exchange process between the aqueous solution and the catalyst layer ionomer. Therefore, in situ polarization curve and cyclic voltammetry data were used as surrogate values for Ca^{2+}. From an ohmic resistance point of view, airborne contaminants do not affect the membrane conductivity. However, the Figure 2b acetonitrile result suggests that a decomposition product is responsible for the change. As for Ca^{2+}, the membrane conductivity is moderately affected at the 5 ppm level. The measurement of the liquid water content inside gas diffusion electrodes is planned and are expected to provide insight into the effect of airborne contaminants' adsorption on their hydrophobic properties. This measurement will not be completed for the foreign cation case as salt precipitation is not expected under automotive conditions (relative humidity <100 %). All contaminants create current redistributions induced by an uneven contaminant concentration distribution over the electrode active area, thus increase risks of local membrane failures in the long term by an increased peroxide generation rate for airborne contaminants or greater pinhole formation probability due to the presence of the foreign ion expulsing water from the membrane and increasing its brittleness. Acetylene, methyl methacrylate and propene are partly or fully oxidized to CO_2 or CO within the fuel cell and cell voltage operating range. This situation explains the gradual and complete performance recovery after the contaminant injection is interrupted and provides an avenue to further accelerate the revival process. The Ca^{2+} ion may precipitate as a salt blocking pores in the gas diffusion electrode and flow field channels, Figure 1b, therefore Ca^{2+} removal in this case is better achieved by keeping and transferring the foreign cation into the aqueous phase.

CONCLUSIONS AND FUTURE DIRECTIONS

- Generally, temperature and contaminant concentration significantly affected fuel cell contamination whereas the current density effect was relatively smaller
- Fuel cell contamination by bromomethane was hardly affected by any operating condition whereas Ca^{2+} widely influenced fuel cell losses with current density
- Contaminant tolerance limits for seven airborne contaminants and one foreign cation, and a fuel cell performance loss of 1% fluctuate from ~0.2 ppm to 800 ppm with the exception of bromomethane
- Complete planned diagnostic tests to support the development of contamination mechanisms and recovery strategies
- Complete long-term tests to assess the impact of increased peroxide production with airborne

TABLE 2. Summary of Ex Situ and In Situ Diagnostic Methods' Results for Seven Airborne Contaminants and One Foreign Cation

Contaminant	Kinetic current (% loss in air at 30°C and 0.9 V vs RHE)	Electrochemical catalyst area (% loss in N_2 at 30°C)	H_2O_2 current (% gain in air at 30°C and 0.5 V vs RHE)[a]	Membrane conductivity (% loss at 80°C and 50 % relative humidity)	GDE water content	Dimensionless local current (maximum % loss and gain in air at 80°C)	Contaminant conversion (% in air at 80°C)[b]
Acetonitrile	85 (16.9 mM)	>60 (16.9 mM)	130 (16.9 mM)	0 (100 ppm)	TBD	TBD	Test completed (analysis ongoing)
Acetylene	100 (4,030 ppm)	>90 (4,040 ppm)	601 to 1027 (4,030 ppm)	1-2 (500 ppm)	TBD	–99 to 100 after 30 min, –17 to 18 at steady state (300 ppm)	0.8 to 100 for 0.55 to 0.85 V (300 ppm)
Bromomethane	54 (400 ppm)	43 (400 ppm)	56 (400 ppm)	-	TBD	–19 to 12 (5 ppm)[c]	TBD
Iso-propanol	12 (1 mM)	7 (1 mM)	18 (1 mM)	-	TBD	TBD	TBD
Methyl methacrylate	72 (1 mM)	65 (1 mM)	350 to 491 (1 mM)	-	TBD	–7 to 6 (20 ppm)	49 to 57 for 0.55 to 0.68 V (20 ppm)
Naphthalene	77 (sat soln)[d]	>90 (sat soln)[d]	171 (sat soln)[d]	-	TBD	TBD	TBD
Propene	53 (1,010 ppm)	38 (1,010 ppm)	604 (1,010 ppm)	-	TBD	–8 to 6 (100 ppm)	43 to 89 for 0.55 to 0.85 V (100 ppm)
Ca^{2+}	21 (5 ppm)[e]	16-46 (5 ppm)[e]	-	1.1-11 (5 ppm)[f]	-	–50 to 20 (5 ppm)[g]	-

[a] The total current is still mostly due to oxygen reduction in spite of a large peroxide production rate increase.
[b] In all cases, observed products include the unaltered contaminant, CO and CO_2.
[c] A steady state was not attained at the end of the contamination period.
[d] 0.25 mM solubility at 25°C.
[e] Derived from in situ polarization curve and cyclic voltammetry tests.
[f] In situ result by current interrupt for 0.6-1 A cm^{-2} and 125 % relative humidity before a steady state is reached at 100 h.
[g] 0.6 rather than 1 A cm^{-2} before a steady state is reached at 100 h.
RHE – reversible hydrogen electrode; GDE – gas diffusion electrode; TBD – to be determined

contaminants and increased membrane brittleness with a foreign cation on fuel cell durability

- Disseminate the large fuel cell contamination database

FY 2013 PUBLICATIONS/PRESENTATIONS

1. J. Qi, X. Wang, U. Pasaogullari, L. Bonville, T. Molter, 'Effect of Al^{3+} Contaminant on Polymer Electrolyte Fuel Cell Performance', *J. Electrochem. Soc*., **160** (2013) F916.

2. M.A. Uddin, X. Wang, J. Qi, M.O. Ozdemir, L. Bonville, U. Pasaogullari, T. Molter, 'Effects of Chloride Contamination on PEFCs', *Electrochem. Soc. Trans*., accepted.

3. J. Qi, X. Wang, M.O. Ozdemir, M.A. Uddin, L. Bonville, U. Pasaogullari, T. Molter, 'Effect of Cationic Contaminants on Polymer Electrolyte Fuel Cell Performance', *Electrochem. Soc. Trans*., accepted.

4. X. Wang, J. Qi, O. Ozdemir, U. Pasaogullari, L.J. Bonville, T. Molter, 'Effect of Ca^{2+} as an Air Impurity on Polymer Electrolyte Fuel Cells', *Electrochem. Soc. Trans*., accepted.

5. J. St-Pierre, J. Ge, Y. Zhai, T.V. Reshetenko, M. Angelo, 'PEMFC Cathode Contamination Mechanisms for Several VOCs - Acetonitrile, Acetylene, Bromomethane, Iso-propanol, Methyl Methacrylate, Naphthalene and Propene', *Electrochem. Soc. Trans*., accepted.

6. Y. Zhai, J. St-Pierre, J. Ge, 'PEMFC Cathode Contamination with Acetylene - Potential Dependency', *Electrochem. Soc. Trans*., accepted.

7. M.A. Uddin, X. Wang, J. Qi, M.O. Ozdemir, L. Bonville, U. Pasaogullari, T. Molter, 'Effects of Chloride Contamination on PEFCs', in *Meeting Abstracts*, Electrochemical Society volume 2013-2, The Electrochemical Society, Pennington, NJ, 2013, abstract 1334 (224^{th} Electrochemical Society meeting oral presentation).

8. J. Qi, X. Wang, M.O. Ozdemir, M.A. Uddin, L. Bonville, U. Pasaogullari, T. Molter, 'Effect of Cationic Contaminants on Polymer Electrolyte Fuel Cell Performance', in *Meeting Abstracts*, Electrochemical Society volume 2013-2, The Electrochemical Society, Pennington, NJ, 2013, abstract 1333 (224^{th} Electrochemical Society meeting oral presentation).

9. X. Wang, J. Qi, O. Ozdemir, U. Pasaogullari, L.J. Bonville, T. Molter, 'Effect of Ca^{2+} as an Air Impurity on Polymer Electrolyte Fuel Cells', in *Meeting Abstracts*, Electrochemical Society volume 2013-2, The Electrochemical Society, Pennington, NJ, 2013, abstract 1332 (224th Electrochemical Society meeting oral presentation).

10. J. St-Pierre, J. Ge, Y. Zhai, T. Reshetenko, M. Angelo, 'PEMFC Cathode Contamination Mechanisms for Several VOCs - Acetonitrile, Acetylene, Bromomethane, Iso-Propanol, Methyl Methacrylate, Naphthalene and Propene', in *Meeting Abstracts*, Electrochemical Society volume 2013-2, The Electrochemical Society, Pennington, NJ, 2013, abstract 1330 (224th Electrochemical Society meeting oral presentation).

11. Y. Zhai, J. St-Pierre, J. Ge, 'PEMFC Cathode Contamination with Acetylene - Potential Dependency', in *Meeting Abstracts*, Electrochemical Society volume 2013-2, The Electrochemical Society, Pennington, NJ, 2013, abstract 1329 (224th Electrochemical Society meeting oral presentation).

12. T. Reshetenko, J. St-Pierre, 'The Impact of Selected Air Pollutants on Spatial PEMFC Performance', in *Meeting Abstracts*, Electrochemical Society volume 2013-2, The Electrochemical Society, Pennington, NJ, 2013, abstract 1328 (224th Electrochemical Society meeting oral presentation).

13. J. Ge, Y. Zhai, J. St-Pierre, 'An RRDE Evaluation of the C_2H_2 Effect on the ORR', in *Meeting Abstracts*, Electrochemical Society volume 2013-2, The Electrochemical Society, Pennington, NJ, 2013, abstract 1302 (224th Electrochemical Society meeting oral presentation).

14. J. St-Pierre, M. Angelo, 'The Effect of Airborne Contaminants on Fuel Cell Performance and Durability', United States Department of Energy 2013 Annual Merit Review meeting, Washington, DC, May 14, 2013.

15. J. St-Pierre, 'The Effect of Airborne Contaminants on Fuel Cell Performance and Durability', US DRIVE Fuel Cell Tech Team meeting, Southfield, MI, November 14, 2012.

REFERENCES

1. J. St-Pierre, 'Air Impurities', in *Polymer Electrolyte Fuel Cell Durability*, Edited by F.N. Büchi, M. Inaba, T.J. Schmidt, Springer, 2009, p. 289.

2. J. St-Pierre, Y. Zhai, M. Angelo, *Int. J. Hydrogen Energy*, **37** (2012) 6784.

3. Y. Zhai, J. St-Pierre, M. Angelo, *Electrochem. Soc. Trans.*, **50**(2) (2012) 635.

4. J. St-Pierre, *Electrochim. Acta*, **55** (2010) 4208.

5. J. St-Pierre, *Int. J. Hydrogen Energy*, **36** (2011) 5527.

6. Y. Zhai, K. Bethune, G. Bender, R. Rocheleau, *J. Electrochem. Soc.*, **159** (2012) B524.